Hydrogen Production from Natural Gas Thermal Cracking: Design and Test of a Pilot-scale Solar Chemical Reactor

S. Rodat, S. Abanades, G. Flamant

This document appeared in

Detlef Stolten, Thomas Grube (Eds.):
18th World Hydrogen Energy Conference 2010 - WHEC 2010
Parallel Sessions Book 3: Hydrogen Production Technologies - Part 2
Proceedings of the WHEC, May 16.-21. 2010, Essen
Schriften des Forschungszentrums Jülich / Energy & Environment, Vol. 78-3
Institute of Energy Research - Fuel Cells (IEF-3)
Forschungszentrum Jülich GmbH, Zentralbibliothek, Verlag, 2010
ISBN: 978-3-89336-653-8

Hydrogen Production from Natural Gas Thermal Cracking: Design and Test of a Pilot-scale Solar Chemical Reactor

Sylvain Rodat, **Stéphane Abanades**, **Gilles Flamant**, Processes, Materials, and Solar Energy Laboratory, CNRS-PROMES, Font-Romeu, France

Solar methane dissociation offers the possibility for the clean co-production of hydrogen and carbon black [1-2]. It appears as an alternative to the steam methane reforming and the furnace process [3] dedicated to the conventional production of hydrogen and carbon black, respectively. The solar process avoids both CO_2 emissions from fossil fuel combustion required to carry out the endothermic reaction and from the reaction of steam reforming. Indeed, the energy supplied by fossil fuel combustion is replaced by concentrated solar energy and methane cracking results in solid carbon and hydrogen only.

Maag et al. [4] developed a direct heating solar reactor seeded with particles. Direct solar heating was also experienced by Kogan et al. [5] with a tornado flow configuration. Indirect heating reactors based on tubular designs were proposed by Dahl et al. [6] and Rodat et al. [7]. The investigation of reaction kinetics was also addressed [8-10]. Nevertheless, the previous developed reactors did not exceed 10 kW scale. In order to acquire more experience towards a potential industrial application, a 50 kW multi-tubular solar reactor was constructed, tested, and simulated. This paper presents the experimental results related to the performances of this pilot-scale solar reactor.

1 Experimental Set-up

The reactor was designed for a nominal power of 50 kW of incident solar power (Figure 1). The reactor body is made of an aluminium shell (800x780x505 mm) and a water-cooled front face with a 13 cm-diameter aperture to let concentrated solar radiation entering within the reactor cavity. The radiations are absorbed by the graphite cavity (360x400x300 mm) that approaches a black body behaviour. To avoid contact of graphite with the oxidizing atmosphere, the opening is protected by a domed quartz window (outer diameter of 360 mm) swept by a nitrogen flow to avoid overheating. The space between the graphite cavity and the aluminium shell is filled with three different insulating layers to limit conduction losses. Seven graphite tubes (800 mm length, 26 mm OD, 18 mm ID) cross the graphite cavity horizontally and they are heated both by direct solar radiation and by IR-radiation from the hot graphite cavity walls. Each tube is fed with a mixture of argon and methane thanks to 2 mass-flow controllers dedicated to each tube (total of 14 mass-flow controllers). Each tube entrance is equipped with an absolute pressure sensor. At the exit, the products (particles and gases) from the tubes are collected and cooled down and then, they are directed towards a filter composed of 6 bags enabling the separation of the carbon black from the gaseous phase that is evacuated to the vent. Before this filter, a sampling pump is used to bypass a part of the products towards a secondary filter for gas analysis. The gas analysis system is composed of an online analyser for measuring hydrogen and methane concentrations (NGA 2000 MLT3) as well as a gas chromatograph (micro GC Varian CP

4900) for quantifying the gas species in the course of the experiment. The temperatures in the reactor are measured by five thermocouples and by one solar blind optical pyrometer (wavelength: 5.14 µm). Two type B thermocouples are set in contact with the graphite cavity, one at the top (B_top), another at the back (B_back). At about the same location, K-thermocouples (K_top and K-back) measure the temperature at a depth of 5 cm (from the aluminium shell surface) in the insulated zone. In addition, a type B thermocouple is inserted 24 cm inside the lowest graphite tube on which the optical pyrometer is also pointing, thus giving a redundant measurement of the reaction zone by two different means.

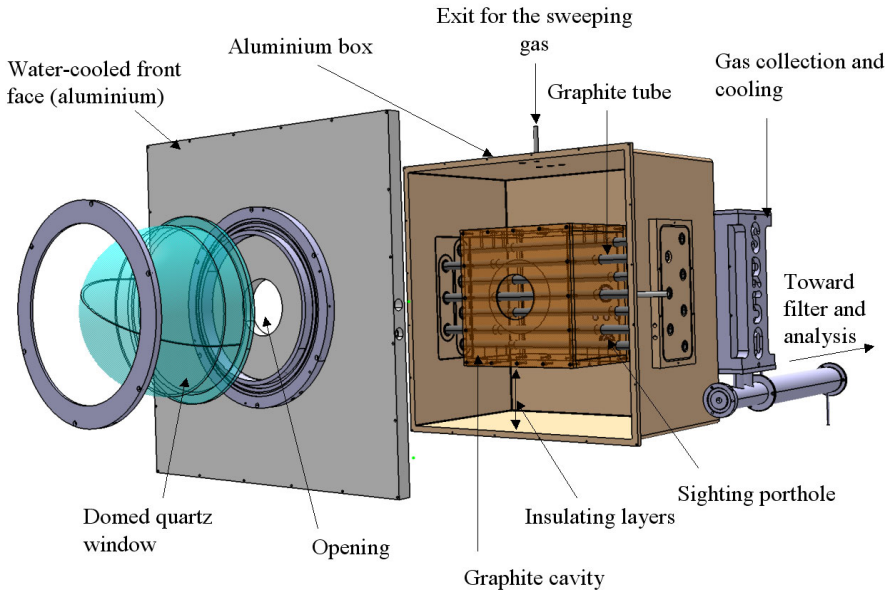

Figure 1: Scheme of the pilot-scale solar reactor.

An experimental run is composed of two steps. The first step is the heating of the reactor under concentrated solar irradiation coming from the 1 MW solar furnace of CNRS-PROMES. During this period, the tubes are fed with pure argon till the targeted temperature is reached. Then, a mixture of argon and methane is injected once the temperature is stabilized and the operating conditions are maintained during about an hour to produce significant amounts of carbon black for further analysis.

2 Experimental Conditions

The experimental conditions are listed in Table 1. Two series were carried out: the first one with 10.5 NL/min of CH_4 and 31.5 NL/min of Ar for temperatures between 1608 K and 1928 K (runs 1 to 5) and the second one with 21 NL/min of CH_4 and 49 NL/min of Ar for temperatures ranging from 1698 K to 1808 K (runs 6 to 8). In the first series, one experimental condition was repeated twice to check the results reproducibility (runs 3 and 4). In the second series, run 7 was repeated with only 21 NL/min of argon dilution (50 % of CH_4 in the feed) instead of 49 NL/min (run 8). After each experimental run at given operating conditions, the carbon was recovered in the filter so that carbon black samples were

representative of specific conditions. About 100 g of sample was recovered for each run and was available for analysis and characterization.

Table 1: Summary of the experimental conditions tested.

Run	Ar (NL/min)	CH_4 (NL/min)	CH_4 mole fraction	Pressure (Pa)	Tpyrometer (K)	Residence time (s)
1	31.5	10.5	0.25	43000	1608	0.070
2	31.5	10.5	0.25	46000	1693	0.071
3	31.5	10.5	0.25	43000	1778	0.063
4	31.5	10.5	0.25	42000	1793	0.061
5	31.5	10.5	0.25	42000	1928	0.057
6	49	21	0.3	47000	1698	0.043
7	49	21	0.3	43000	1808	0.037
8	21	21	0.5	41000	1798	0.059
9	49	21	0.3	45000	1873	0.038

3 Experimental results

Figure 2 shows typical measurements of temperatures, H_2 and CH_4 off-gas mole fractions, DNI (Direct Normal Irradiation) recorded for the experimental run 2. It can be decomposed in three experimental stages: heating of the reactor in Ar, cracking period (methane injection), and passive cooling of the reactor (no solar irradiation).

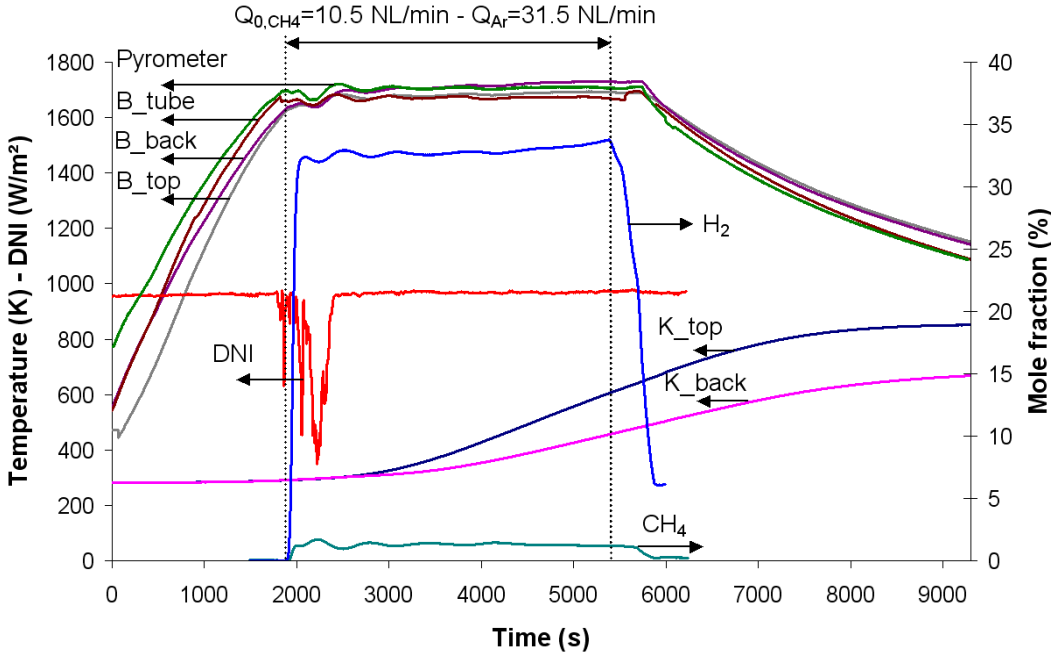

Figure 2: Online monitoring of temperatures, DNI, H_2 and CH_4 off-gas mole fractions.

After a heating period of about 40 min under an argon flow in the tubes, the temperature of the reactor reaches 1700 K. All the temperature sensors tend to a similar measured temperature ranging between 1670 K and 1720 K. The highest temperature is given by the pyrometer that points directly on the outer wall of a tube. It can be stated that the temperature is homogeneous around the cavity during the methane splitting period. When the targeted temperature is reached and stabilized, 31.5 NL/min of argon and 10.5 NL/min of methane are injected. H_2 is rapidly detected at the exit along with residual CH_4 (not dissociated). After 2400 s of isothermal experiment, the H_2 mole fraction in the off-gas increases slightly as a result of tubes clogging. Carbon deposit in the tubes causes a pressure increase and thereby a residence time increase that favours better CH_4 and C_2H_2 dissociation. After about one hour of isothermal experiment, the tubes are successively stopped because of their progressive blocking.

The reactor performances are given in terms of methane conversion, hydrogen yield, and carbon yield:

$$X_{CH_4}=\frac{F_{0,CH_4}-F.y_{CH_4}}{F_{0,CH_4}};\quad Y_{H_2}=\frac{F.y_{H_2}}{2.F_{0,CH_4}};\quad Y_C=\frac{F_{0,CH_4}-(F.y_{CH_4}+2.F.y_{C_2H_2}+2.F.y_{C_2H_4}+2.F.y_{C_2H_6})}{F_{0,CH_4}}$$

where $F_{0,CH4}$ is the inlet molar flow-rate of CH_4, y_i is the mole fraction of species i, and F is the total outlet flow-rate (including argon as buffer gas) obtained from:

$F = F_{Ar}/(1-\Sigma y_i)$ (F_{Ar} is the molar flow-rate of Ar)

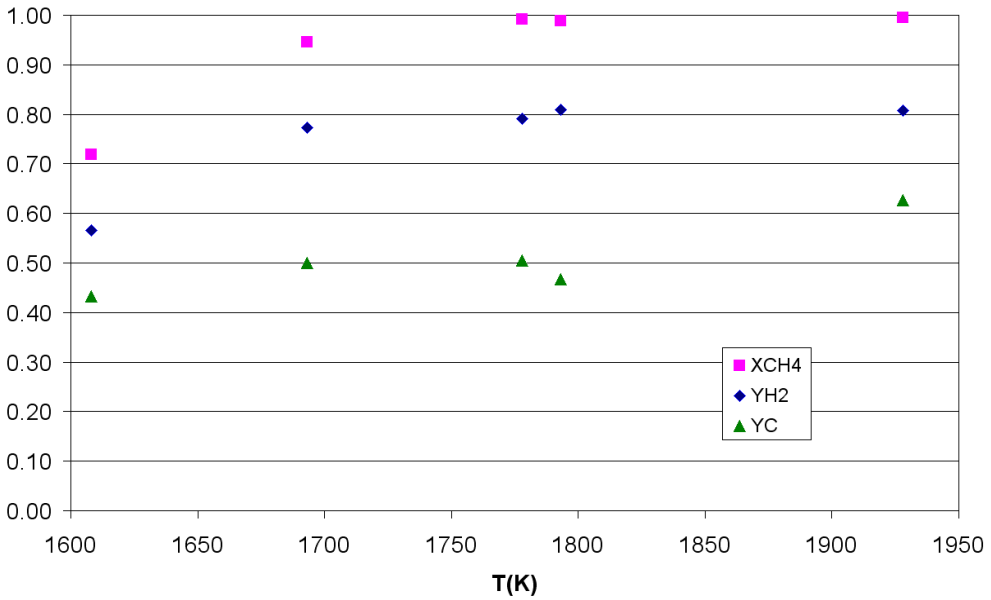

Figure 3: CH_4 conversion, H_2 yield, and C yield versus temperature for the first experimental series (Ar: 31.5 NL/min, CH_4: 10.5 NL/min).

Figure 3 shows the results concerning the first experimental series (Ar: 31.5 NL/min, CH_4: 10.5 NL/min) in terms of methane conversion, hydrogen yield, and carbon yield with increasing temperatures (1608 K-1928 K). The higher the temperature, the better the chemical performance. Moreover, the CH_4 conversion is always higher than the H_2 yield and

the C yield. Since the conversion of CH_4 into C_2H_2 leads to the production of 1.5 mole of H_2 per mole of CH_4 without carbon production, the H_2 yield is higher than the C yield. The intermediate C_2H_2 mainly affects the carbon yield. For temperatures above 1778 K, complete methane conversion is achieved.

Figure 4 shows the results related to the second experimental series (Ar: 49 NL/min, CH_4: 21 NL/min) in the temperature range 1698 K-1873 K. Similar trends are observed for the temperature influence but the CH_4 conversion never reaches completion even for temperatures up to 1873 K as a result of higher flow-rates than the first series. For the run #8 (50 % of CH_4 in the feed), better chemical performances are obtained due to a higher residence time as a result of the lower argon dilution (Ar: 21 NL/min instead of 49 NL/min). The comparison between the results of the first and second series shows enhanced performances for the first series, which points out again the strong influence of the residence time. Residence time and temperature thus appear as the most critical parameters.

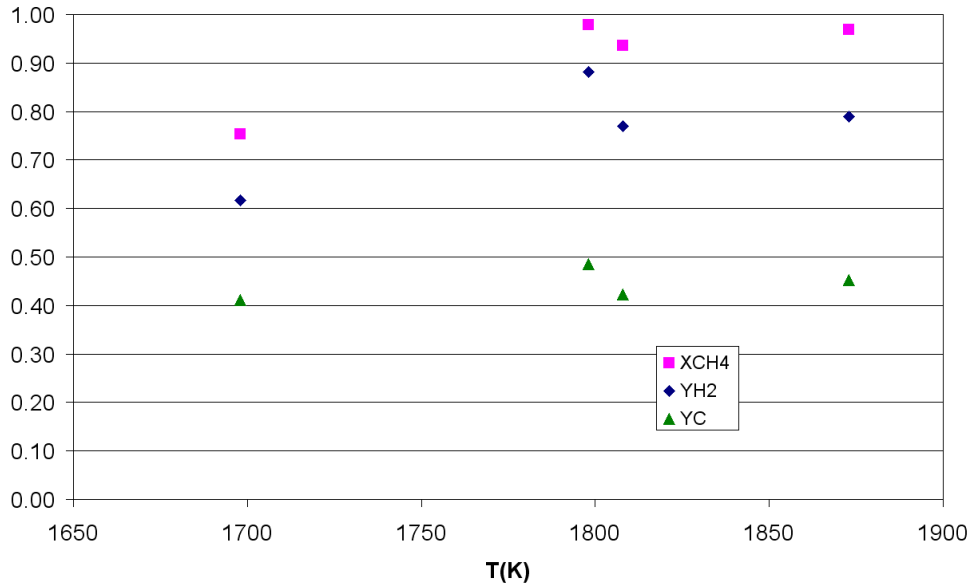

Figure 4: CH_4 conversion, H_2 yield, and C yield versus temperature for the second experimental series (CH_4: 21NL/min).

Acknowledgements

This study was funded by the European Project SOLHYCARB (2006-2010, Contract SES-CT2006-19770). The authors wish to thank O. Prévost, M. Garrabos, and J.L. Sans for their technical support during the solar reactor manufacturing and operation.

References

[1] P.L. Spath, W.A. Amos, Using a concentrating solar reactor to produce hydrogen and carbon black via thermal decomposition of natural gas: feasibility and economics, Journal of Solar Energy Engineering, 125(2), 2003, 159-164.

[2] T. Pregger, D. Graf, W. Krewitt, C. Sattler, M. Roeb, S. Möller, Prospects of solar thermal hydrogen production processes, International Journal of Hydrogen Energy, 34(10), 2009, 4256-4267.

[3] F.C. Lockwood, J.E. Van Niekerk, Parametric Study of a Carbon Black Oil Furnace, Combustion and Flame, 103(1-2), 1995, 76-90.

[4] G. Maag, G. Zanganeh, A. Steinfeld, Solar thermal cracking of methane in a particle-flow reactor for the co-production of hydrogen and carbon, International Journal of Hydrogen Energy, 34, 2009, 7676-7685.

[5] M. Kogan and A. Kogan, Production of hydrogen and carbon by solar thermal methane splitting. I. The unseeded reactor, International Journal of Hydrogen Energy, 28(11), 2003,1187-1198

[6] J. K. Dahl, K. J. Buechler, A. W. Weimer, A.Lewandowski and C. Bingham, Solar-thermal dissociation of methane in a fluid-wall aerosol flow reactor, International Journal of Hydrogen Energy, 29(7), 2004, 725-736.

[7] S. Rodat, S. Abanades, G. Flamant, High-Temperature Solar Methane Dissociation in a Multitubular Cavity-Type Reactor in the Temperature Range 1823-2073 K, Energy & Fuels, 23, 2009, 2666-2674.

[8] J.K. Dahl, V.H. Barocas, D.E. Clough, A.W. Weimer, Intrinsic kinetics for rapid decomposition of methane in an aerosol flow reactor, International Journal of Hydrogen Energy, 27(4), 2002, 377-386.

[9] S. Rodat, S. Abanades, J. Coulié, G. Flamant, Kinetic modelling of methane decomposition in a tubular solar reactor, Chemical Engineering Journal, 146(1), 2009, 120-127.

[10] M. Younessi-Sinaki, E.A. Matida, F. Hamdullahpur, Kinetic model of homogeneous thermal decomposition of methane and ethane, International Journal of Hydrogen Energy, 34(9), 2009, 3710-3716.